Auroras observations of the MAIN in Apatity during 2014/15 winter season

Veneta Guineva [1], Irina Despirak [2], Boris Kozelov [2]

[1] Space Research and Technology Institute, BAS, Stara Zagora Department, Bulgaria
[2] Polar Geophysical Institute (PGI), Apatity, Murmansk region, Russia

E mail (v_guineva@yahoo.com).

Accepted: 16 March 2017

Abstract. In this work we review substorms, originated during the 2014/2015 winter season. Observations of the Multiscale Aurora Imaging Network (MAIN) in Apatity have been used. Solar wind and interplanetary magnetic field parameters were estimated by the 1-min sampled OMNI data base from CDAWeb (http://cdaweb.gsfc.nasa.gov/cdaweb/istp_public/). Auroral disturbances were verified by the 10-s sampled data of IMAGE magnetometers and by data of the all-sky camera at Apatity. Subject of the review were the peculiarities in the development of substorms occurred during different geomagnetic conditions. The behavior of the substorms developed in non-storm time and during different phases of geomagnetic storms was discussed.

Key words: solar wind, substorms, auroras

Introduction

One of the factors of the space weather is the magnetetospheric substorms excitation in the night sector of the auroral latitudes. It is known that the substorm onset and development differ during various conditions of the solar wind (e.g., Gerard et al., 2004; Gussenhofen, 1982; Yahnin et al., 2004). In particular, solar wind parameters influence the substorm intensity, the latitudinal and longitudinal substorm features (substorm onset location, substorm extent), the occurrence of substorms at high geomagnetic latitudes (e.g. Nishida 1971; McPherron 1973; Loomer and Gupta 1980; Dmitrieva and Sergeev 1984; Despirak et al. 2008; Despirak et al. 2014).

Moreover, disturbances in the solar wind, namely magnetic clouds (MC) and the regions in front of flows in the solar wind (CIR and Sheath) can often cause geomagnetic storms. Geomagnetic storms differ also by their intensity, by the duration of the recovery phase and other parameters (for example CIR-storms and MC- or Sheath-storms) (Huttunen et al., 2006; Pulkkinen et al., 2006; Yermolaev and Yermolaev, 2006; Tsurutani et al., 2006). It should be noted also that there are more complicated storm cases, when the magnetic storms are caused by several sources in the solar wind, coming consecutively one after another or partly overlapping. For example, there are two events of strong geomagnetic activity on 7-17 March 2012 and 17-20 March 2015 (Tsurutani et al., 2014; Maris et al., 2014; Guineva et al, 2016). Thus, substorms could be observed under different interplanetary conditions: during the passage of different solar wind streams and structures by the Earth, during development of different geomagnetic storms, as well as in quiet conditions.

The goal of this work is to review substorm developments during different phases of geomagnetic storms and in non-storm time using measurements of the camera system MAIN in Apatity during 2014/2015 observational winter season.

Instrumentation and Data Used

Measurements from the Multiscale Aurora Imaging Network (MAIN) in Apatity during 2014/2015 observational season have been used. The cameras observational system has being built in Apatity since 2008. It is described in detail by Kozelov et al., 2012. Apatity is settled at auroral latitudes. Its geographic coordinates are: 67.58°N, 33.31°E, and the corrected geomagnetic ones – 63.86°N, 112.9°E. The cameras observational system comprises 4 auroral cameras with different fields of view providing simultaneous observations from spatially separated points.

To analyze auroral phenomena we used both individual cameras images and keograms. A keogram is a time versus latitude (or zenith angle) plot of the intensity derived from the individual images. Keograms give information about the progress of the auroral activity. The name "keogram" comes from the old Eskimoan word "keoitt" meaning "aurora borealis". The keograms are created by extracting pixel columns in N-S direction (where North may be the geographic or magnetic one) from consecutive individual camera images and putting these columns side by side.

To study the substorm development data from the Apatity all-sky camera (images and keograms) and the Guppy F-044C (GC) camera with field of view ~67° (keograms), part of the observational system MAIN, were used. In the all-sky images the central column corresponds to the North-South latitudinal cross section of the auroral zone. These columns from each image within 1-hour interval have been used to construct an all-sky keogram (Kozelov et al., 2012). The GC camera data were corrected regarding the exposition time, the gain, the heterogeneity of the dark field, and the objective transmittance change depending on the angle of observation. The keograms were built in

direction magnetic North (up) (Guineva et al, 2016). For the examined substorms the N-S pixel columns from the images within 20-min. interval including the substorm onset and further development were used to construct the keograms. The vertical axis is the zenith angle. The zero angle coincides with zenith.

Solar wind and interplanetary magnetic field parameters were taken from the 1-min sampled OMNI data base of the CDAWeb (http://cdaweb.gsfc.nasa.gov/cgi-bin/eval2.cgi).

Auroral geomagnetic disturbances were verified by the ground-based data of IMAGE magnetometers network (using the meridional TAR-NAL and MEK-NOR chains (Tartu (TAR), GMLat. = 54.47°- Ny Ålesund (NAL), GMLat. = 75.25°; Mekrijärvi (MEK), GMLat. = 59.10°; Nordkapp (NOR), GMLat. = 67.73°) and by data of Loparskaya and Lovozero (GMLat. =65.43°; GMLat. =64.23°;) magnetometers.

Auroras disturbances were taken from the data of the Apatity all-sky camera (images and keograms) and the Guppy F-044C (GC) camera (keograms). The measurements during the 2014/2015 season were examined together with the interplanetary conditions during the measuring periods.

During the winter observational season, from September 2014 to April 2015, 10 magnetic clouds (MC) and 25 high speed streams (HSS) were detected. In this time interval 21 geomagnetic storms with SYM/H_{min}< -50 nT occurred. During the 2014/2015 season the Apatity all-sky camera registered 61 substorms and their intensifications.

Below we are going to present 3 examples of substorm observations in Apatity by all-sky camera and Guppy-C camera. One of the examples shows the observations during storm conditions and two examples present the observations in non-storm conditions – during just quiet conditions and during the passage of different solar wind structures beside the Earth, which didn't cause geomagnetic storms.

Results

From September 2014 to April 2015, during the 2014/2015 observational season 61 substorms were identified during clear sky measurements. For the study the substorms were divided into two groups: substorms observed during geomagnetic storms and substorms in non-storm conditions. Our classification of the substorms and their number in the different groups are presented in Table 1. Every group included several sub-groups. The substorms during geomagnetic storms can occur during the main storm phase or during the recovery phase. The recovery phase was divided in near recovery phase and late recovery phase. Another sub-group of the first group was also introduced, namely "structured recovery phase", when the SYM/H index behavior was highly structured. Such cases refer to the so-called "pulsing" or "complicated" storms, when the storm recovery phase is complex, with several relatively deep minima in the SYM/H index. It has to be noted that in this work we don't examine the division of storms by their sources (e.g. CIR-storms, Sheath-, MC- or Ejecta-storms), we confine ourselves just to the examination of storm and non-storm conditions.

The substorms during non-storm conditions were classified as substorms under quiet conditions, when no structures in the solar wind were observed, and as substorms happened when structures in the solar wind near Earth were detected, but these structures didn't provoke geomagnetic storms (see Table 1).

Further three events during the geomagnetic storm on 24 December 2014 and under non-storm conditions on 1 December 2014 and on 27 March 2015 are presented as examples.

Interplanetary conditions in the time interval 19-27 December 2014

Figure 1 presents the solar wind conditions taken from the OMNI database for the interval 19-27 December 2014. This time interval depicts very complicated interplanetary conditions, when several different solar wind structures – magnetic clouds, high speed streams and regions of compressed plasma in front of such flows were overlapped. The OMNI data show some sharp fronts corresponding to the boundaries between Sheath, MCs, CIR and HSS.

In this work, we will not examine in detail the solar wind structures observed during 21 – 24 December 2014 and we will not determine which of them provoked the storms. We would only mention that this complicated case comprising the overlapping of several solar wind structures led to the development of two geomagnetic storms – on 21 and 23 December 2014. Besides, the storm on 21 December 2014 can be considered as "classical" with simple recovery phase, and the storm on 23 December 2014 can be assigned to the so-called "pulsing" storms with structured recovery phase.

During the second storm the SYM/H index reached a minimum of -52 nT at 01:38 UT on 24.12.2014. A long lasting recovery phase (for several days) with 3 consecutive minima was observed. Another characteristic of the recovery phase of this storm was that it was highly structured or irregular. The SYM/H index variations reached about 50% of its range and the minima were close to the deepest one (-52 nT) (Fig.1).

8 substorms were registered by the MAIN system in Apatity during this storm:

1) 00:29:30 UT, 24.12.2014, during the structured minimum, SYM/H=-45 nT
2) 01:16 UT, 24.12.2014, during the structured minimum, SYM/H=-50 nT
3) 16:28:50 UT, 24.12.2014, during the structured recovery phase, SYM/H=-25 nT
4) 19:19:50 UT, 24.12.2014, during the structured recovery phase; SYM/H=-39 nT
5) 20:11 UT, 25.12.2014, during the structured recovery phase SYM/H=-11 nT
6) 23:08 UT, 25.12.2014, near the structured minimum, SYM/H=-35 nT

7) 00:40 UT, 26.12.2014, near the structured minimum, SYM/H=-40 nT
8) 19:32 UT, 26.12.2014, during the structured recovery phase, SYM/H=-33 nT

Below we are going to present 2 examples of substorm observations, namely events number 3 and 4.

Substorm observation on 24 December 2014, 16:28:50 UT

The development of the substorm on 24 December 2014 at 16:28:50 UT is presented in Fig.2.

The substorm was observed during the late structured recovery phase of the storm, the main phase of this storm was observed from ~19 UT on 23 December 2014, at the beginning of a high speed stream (HSS) of the solar wind to 01:38 UT on 24 December 2014. This substorm was observed during the interval when SYM/H index was recovering from its minimum value and at the moment of substorm onset the value of SYM/H index was -25 nT. According to the observations of the chain of magnetic stations IMAGE, the magnetic disturbance spread from Oulujärvi station (OUJ) at CGM Lat.= 60.99°N to Bear Island station (BJN) at CGM Lat.= 71.45°N (the picture of the magnetic disturbances by IMAGE magnetometers is not presented here). The substorm was seen first in the all-sky images at 16:28:50 UT to the North from the station zenith. It is seen that the auroras moved to South, reached zenith and moved further to South. The bright substorm auroras reached the GC camera field of view (15°N) at 16:48 UT. The maximal relative intensity in the field of view was 160 rel. units.

Substorm on 24 December 2014, 19:19:50 UT

The auroras dynamics according to the all-sky and GC cameras data during the substorm on 24 December 2014 at 19:19:50 UT is shown in Figure 3.

This substorm was observed also during the late structured recovery phase of the storm on 23 December. But in the interval ~18:00 – ~ 20:00 UT the SYM/H index decreased to a new minimum, that means a new geomagnetic disturbance. The value of SYM/H index at the moment of substorm onset was ~ -39 nT. By the magnetic stations IMAGE, the magnetic disturbance began at Nurmijärvi station (NUR) at CGM Lat.= 56.89°N and moved to Hornsund station (HOR) at CGM Lat.= 74.13°N, so it covered a larger latitudinal region than the disturbance in the first presented case. In auroras the substorm began in Apatity at 19:19:50 UT. It is seen that substorm auroras appeared in the South part of the field of view. Then auroras travelled northward, surpassed the station zenith and covered the whole field of view. It should be noted that two intensifications of this substorm were observed: at 19:19:50 and at 19:32:40. In the GC keograms the substorm auroras were seen first at 19:24:40 UT for a few minutes (the first intensification) and once again at 19:35:40 UT (the second substorm intensification).

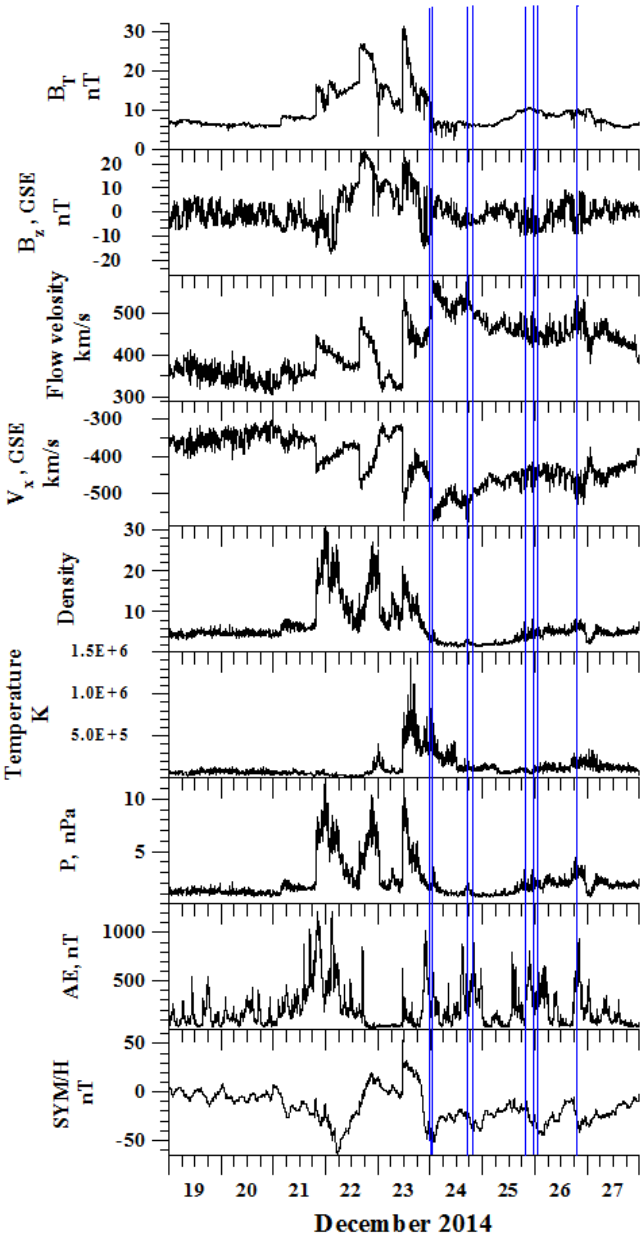

Figure 1. Solar wind and IMF parameters, AE and SYMN/H indices during December 19-27, 2014. From top to bottom: interplanetary magnetic field magnitude BT and the IMF BZ component, the stream velocity V, the X-component of the solar wind velocity VX, the density N, the temperature T, the solar wind dynamic pressure P, the geomagnetic indices AE and SYMN\H. The onsets of the 8 substorms according to the IMAGE magnetometers network and the all-sky camera in Apatity are marked by blue vertical lines.

The maximal relative intensity in the GC camera field of view was 160 rel. units.

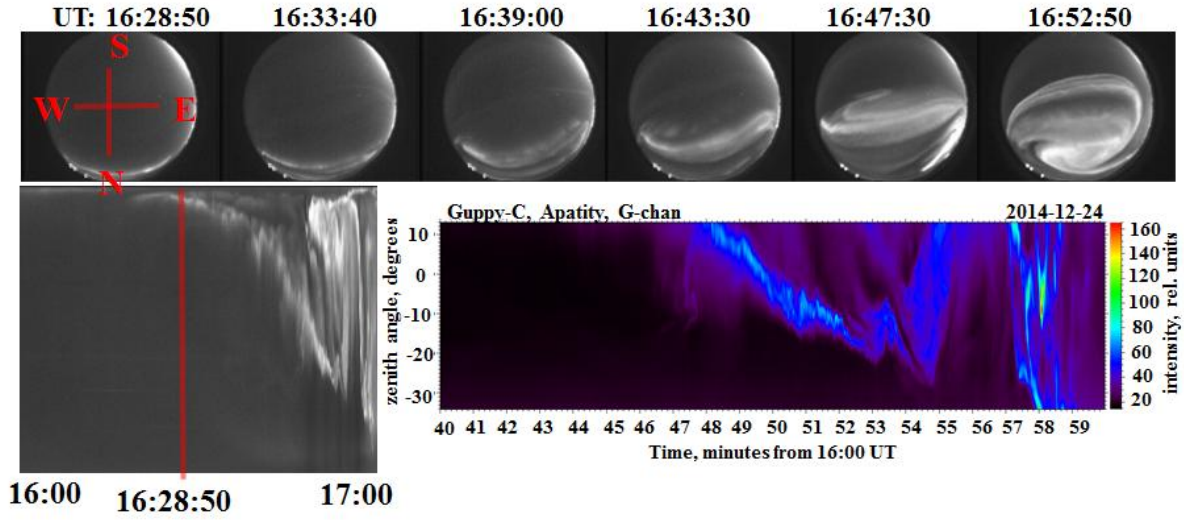

Figure 2. Auroras dynamics during the substorm on 24 December 2014 at 16:28:00 UT according to the all-sky and GC cameras data. The top panel shows some all-sky camera images taken during this substorm (from 16:28:50 to 16:52:50 UT). The left bottom panel presents the all-sky keogram from 16:00 to 17:00 UT and the right bottom panel shows the Guppy (GC) camera keogram from 16:40 to 17:00 UT. The world directions are marked in the first image of the top panel; the universal time is written above each image. The substorm onset is indicated in the all-sky keogram by red vertical line.

Table 1. Classification of the observation conditions during 2014/2015 winter season.

Substorms during geomagnetic storms:	**24**	Substorms during non-storm conditions:	**37**
Main phase	**9**	Quiet conditions	**13**
Near recovery phase	**8**	Non-storm conditions with structures in the solar wind	**24**
Late recovery phase	**3**		
Structured recovery phase	**4**		

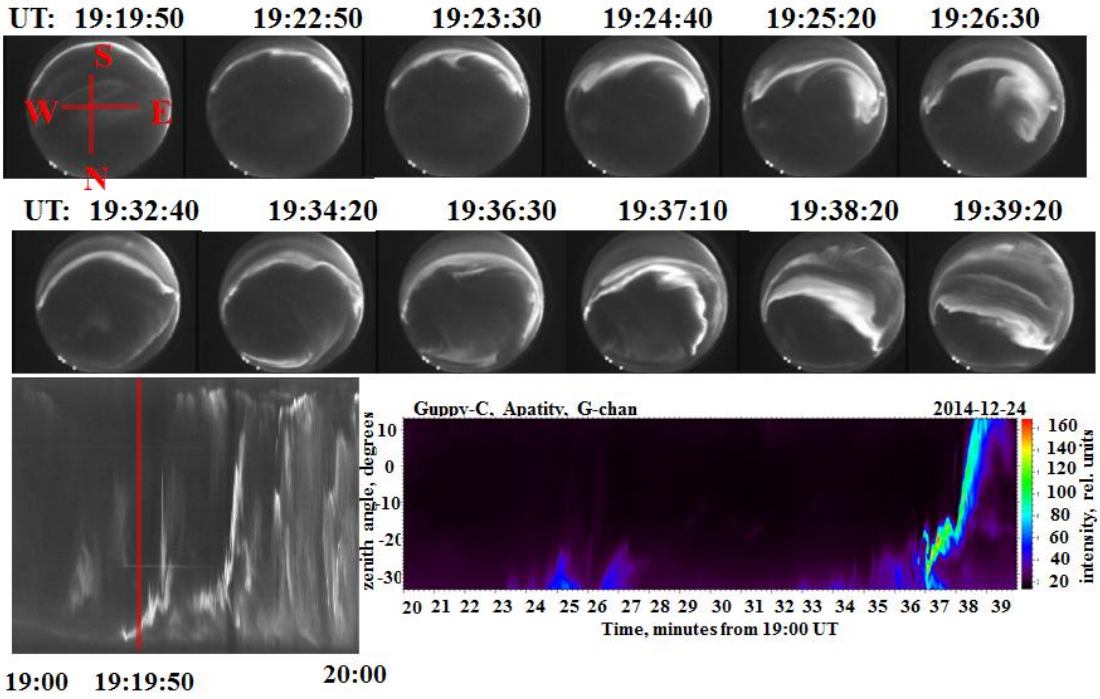

Figure 3. Auroras dynamics during the substorm on 24 December 2014 at 19:19:50 UT. The upper row of the top panel shows some all-sky camera images taken during during the first intensification of this substorm (from 19:19:50 to 19:26:30 UT); the lower row of the top panel shows a second substorm intensification (from 19:32:40 to 19:39:20 UT). The left bottom panel presents the all-sky keogram from 19:00 to 20:00 UT and the right bottom panel shows the GC camera keogram from 19:20 to 19:40 UT. The symbols and designations are the same as the ones in Figure 2.

Interplanetary conditions in the time interval 20-27March 2015

Figure 4 presents the solar wind and IMF parameters, AE and SYM/H indices during 20-28 March 2014. This event is an example of quiet solar wind conditions, which were observed at the end of a solar wind high speed stream (HSS). It should be noted that these are comparatively quiet conditions, but after very strong geomagnetic disturbances. It is known that on 17-18 March 2015 a storm which was one of the strongest geomagnetic storms of SC24, the so-called "St. Patrick's Day 2015 Event" was observed. We have already discussed the substorms observations in Apatity in this disturbed period in a previous paper (Guineva et al, 2016). In this work we considered substorms observations on 26-27 March 2015. From Figure 4 it is seen that a high speed stream was observed in the period 20-25 March.

After that the solar wind velocity decreased from high to low values, and the values of other solar wind parameters (the proton density, the temperature and the dynamic pressure) were low on 26-27 March 2015. The interplanetary magnetic field magnitude was ~5-7 nT, the IMF B_Z component varied in a narrow range near 0, the SYM/H index was ~-15 nT.

3 substorms were registered by the MAIN system in Apatity during 26-27 March 2015:

1) 21:50 UT, 26.03.2015, during quiet conditions, at the end of HSS, SYM/H=-15 nT
2) 23:14 UT, 26.03.2015, during quiet conditions, at the end of HSS, SYM/H=-15 nT
3) 21:31 UT, 27.03.2015, during quiet conditions, after HSS, SYM/H=-12 nT

One example of substorm observations, namely event number 3 is presented below.

Substorm on 27 March 2015, 21:31:30 UT

The aurora dynamics during the substorm on 27 March 2015 according to the all-sky camera data is shown in Figure 5.

The substorm onset occurred at 21:31:30 UT on 27 March 2015 to the North from Apatity. This was an event during quiet interplanetary conditions, and the auroras stayed in the Northern part of the field of view. According to the observations of the IMAGE magnetometers, the magnetic disturbance spread from Pello station (PEL) at CGM Lat.= 63.55°N to Bear Island station (BJN) at CGM Lat.= 71.45°N (the picture of the magnetic disturbances is not presented here).

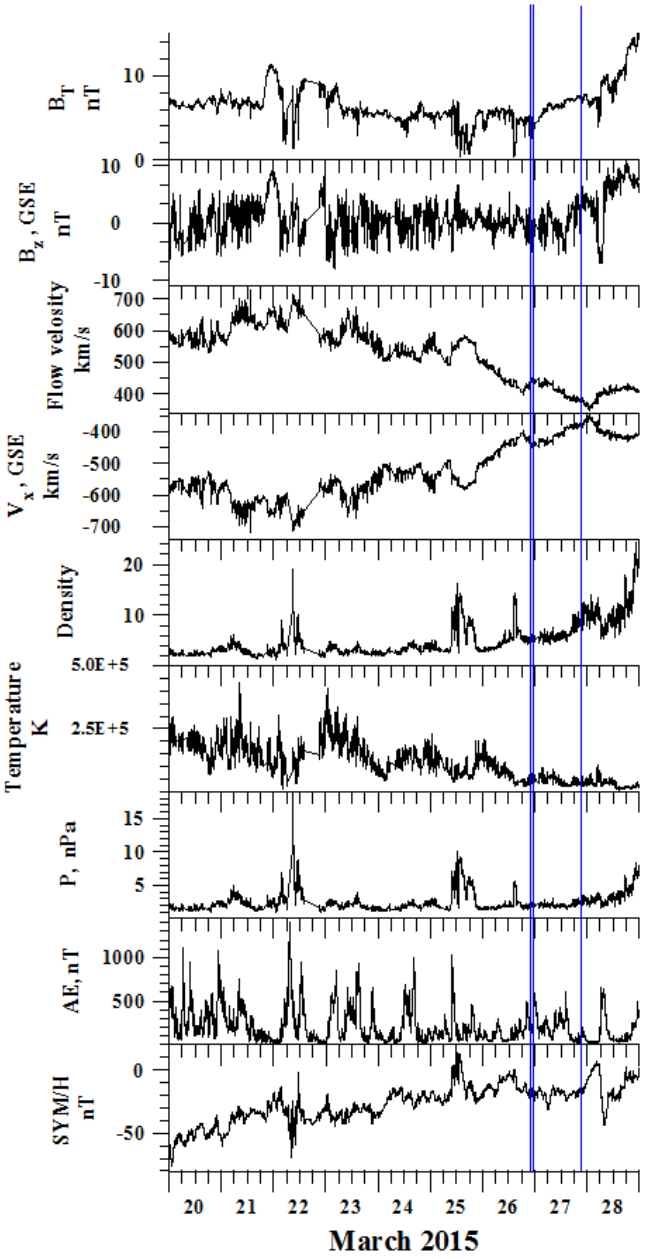

Figure 4. Solar wind and IMF parameters, AE and SYM/H indices during 20-28 March 2014. This is an example of quiet solar wind conditions, after a HSS in the solar wind. The onsets of the 3 substorms according to the IMAGE magnetometers network and the all-sky camera in Apatity are marked by blue vertical lines. The format of Figure 4 is the same as the one of Figure 1.

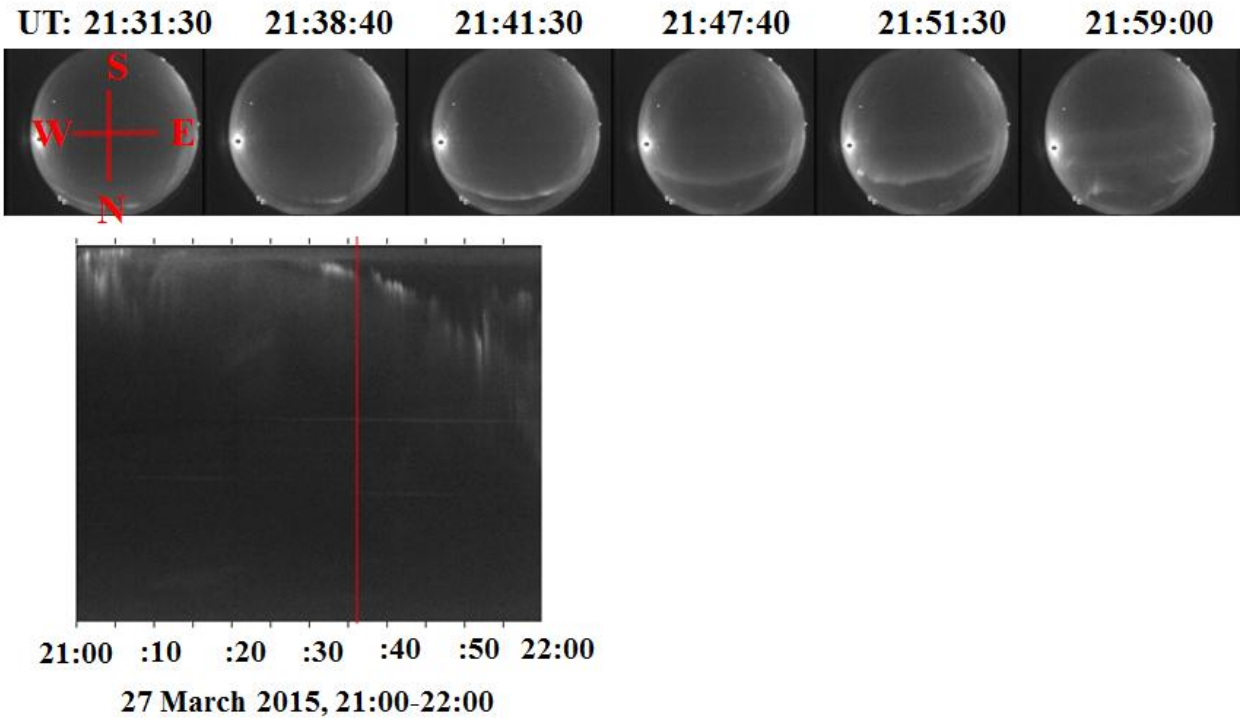

Figure 5. Substorm development on 27 March 2015 at 21:31:30 UT according to the all-sky camera data. The top panel shows some all-sky camera images taken during the substorm (from 21:31:30 to 21:59:00 UT). The bottom panel presents the all-sky keogram from 21:00 to 22:00 UT. The symbols and designations in Figure 5 are the same as the ones in Figure 2.

Interplanetary conditions in the time interval 01-03 December 2014

Figure 6 presents the solar wind and IMF parameters, AE and SYM/H indices during 01-03 December 2014. This is an example of non-storm, conditions, when a high speed stream (HSS) was detected in the solar wind. HSS was observed from ~12 UT on 01 December to ~12 UT 02 December. Although the solar wind speed reached high values (~590 km/s), a geomagnetic storm didn't develop. The SYM/H index was positive before the HSS, the HSS provoked a sharp decrease in SYM/H and its value fluctuated in the range 0 ÷ -15 nT during the HSS. We consider this case as an example of non-storm conditions with structures in the solar wind. Two substorms were registered by the MAIN system in Apatity during 01-03 December 2014, just during the sharp decrease of SYM/H, at the beginning of HSS. Below we are going to present one of them as example.

Substorm on 01 December 2014, 22:22:20 UT

The aurora dynamics during the substorm on 01 December 2014 according to the all-sky camera data is shown in Figure 7. According to the observations of the IMAGE magnetometers, the magnetic disturbance spread from Pello station (PEL) at CGM Lat.= 63.55°N to Bear Island station (BJN) at CGM Lat.= 71.45°N (the picture of the magnetic disturbances is not presented here).

The substorm onset by all-sky camera occurred at 22:22:20 UT to the North from Apatity, then auroras moved to South and reached zenith in 22:23:50 UT. This is an event during non-storm interplanetary conditions, when a structure in the solar wind (HSS) was passing by the Earth. At the onset time the SYM/H value was -6 nT, but this time coincided with the sharp decrease in SYM/H. During this event in non-storm interplanetary conditions the substorm auroras movement from the North boundary of the field of view to South to the station zenith was seen.

Discussion

We studied the substorms, observed by the cameras system MAIN in Apatity during 2014/2015 winter observational season. It is well known that the substorm onset occurs at the South boundary of the auroral oval (e.g.Akasofu, 1964). It is known also that under disturbed geomagnetic conditions the auroral oval expands to lower latitudes, up to 50° geomagnetic latitude ("expanded oval"), under moderate disturbance the auroral oval lies at "auroral" latitudes – 65-67° geomagnetic latitude ("normal oval") and during quiet conditions the auroral oval shrinks to higher latitudes, above 70° ("contracted oval") (Feldstein and Starkov, 1967). The observations by the MAIN system in Apatity confirm this typical

morphology. During disturbed conditions the auroral oval was situated equatorward from Apatity, and during quiet conditions – poleward from Apatity. We made a classification of the registered substorms depending on the interplanetary and geomagnetic conditions (see Table 1 and its explanation). So, during disturbed conditions: during the main storm phase, during the near recovery phase and in some cases during the structured recovery phase the substorm onset occured to the South of Apatity and during the substorm expansion the movement of auroras in South-North direction over Apatity was observed.

And under non-storm conditions: during quiet conditions, during the late storm recovery phase and in some cases when structures in the solar wind were observed or during a structured storm recovery phase the substorm originated to the North from Apatity and the travel of the auroras in North-South direction can be seen. These results confirm our previous studies (Guineva et al., 2016). An important indicator of the level of geomagnetic activity is the geomagnetic SYM/H index (1-min. index expressing the disturbance of the mid-latitude geomagnetic field parallel to the geomagnetic dipole axis). The boundary between substorms occured to the South from Apatity (63.86°N corrected geomagnetic latitude) and to the North from the station zenith in terms of SYM/H index is in the range 35-50 nT.

The maximal relative intensity of the substorm features in the GC camera field of view is considerably larger for substorms occured to the South from Apatity and smaller for substorms arised in zenith or to the North from Apatity.

Conclusions

1. For substorms during the main storm phase or near the SYM/H minimum, auroras occurred to the South of Apatity, and auroras expansion in North direction was observed.
2. For substorms during the late recovery phase or under quiet interplanetary conditions, auroras were observed near the station zenith or to the North of the station, and their motion from the North to the South was registered.
3. The boundary between these two types of substorm observations in terms of SYM/H index is in the range 35-50 nT. Therefore, for substorms during a structured storm recovery phase or during "non-storm conditions with structures of solar wind" auroras may occur to the South or to the North from the station zenith depending mainly on the SYM/H value.
4. The maximal relative intensity of the substorm features in the camera field of view is considerably larger during the substorms arised to the South from Apatity.

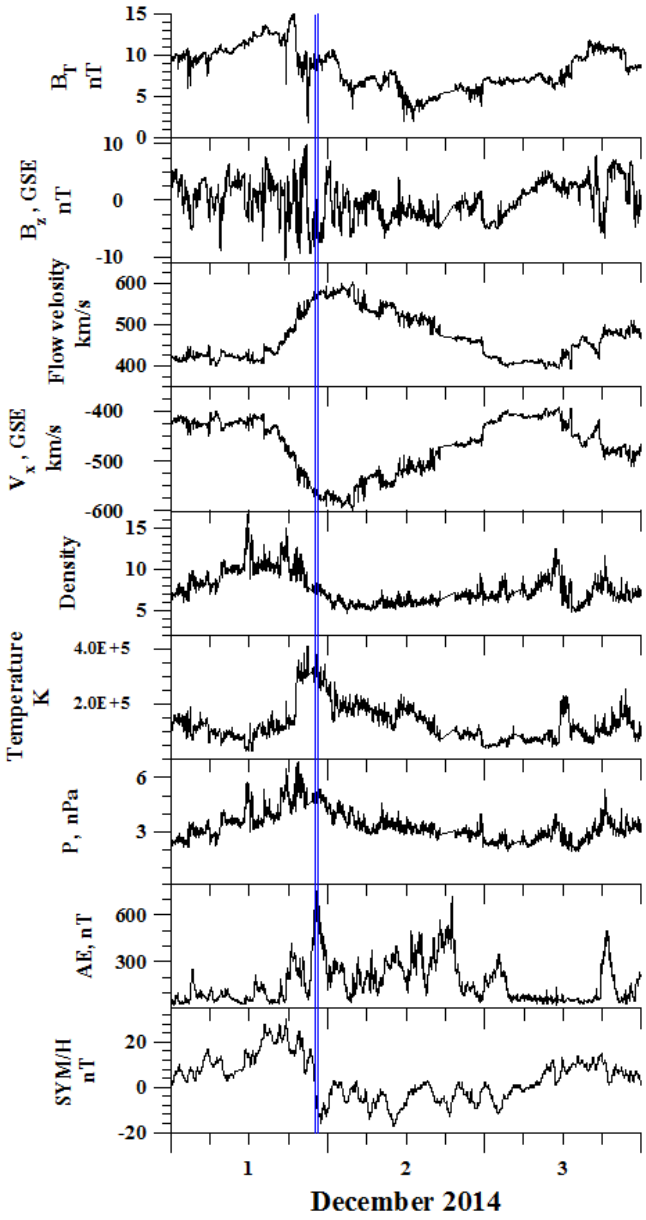

Figure 6. Solar wind and IMF parameters, AE and SYM/H indices during 01-03 December 2014. This is an example of non-storm conditions, but with the presence of a HHS in the solar wind. The onsets of the 2 substorms according to the IMAGE magnetometers network and the all-sky camera in Apatity are marked by blue vertical lines. The format of Figure 6 is the same as the one of Figure 1.

Acknowledgements.

WIND data used in this study were taken from OMNI through http://cdaweb.gsfc.nasa.gov/cdaweb/istp_public/. We are grateful to J. N. King and N. Papatashvili, the heads of the experiments conducted with these instruments. The paper was partly supported by Program No 7 of the Presidium of the Russian Academy of Sciences (RAS). The study is also a part of a joint Russian - Bulgarian Project 2-14 of PGI RAS and IKIT-BAS under the Fundamental Space Research Program between RAS and BAS.

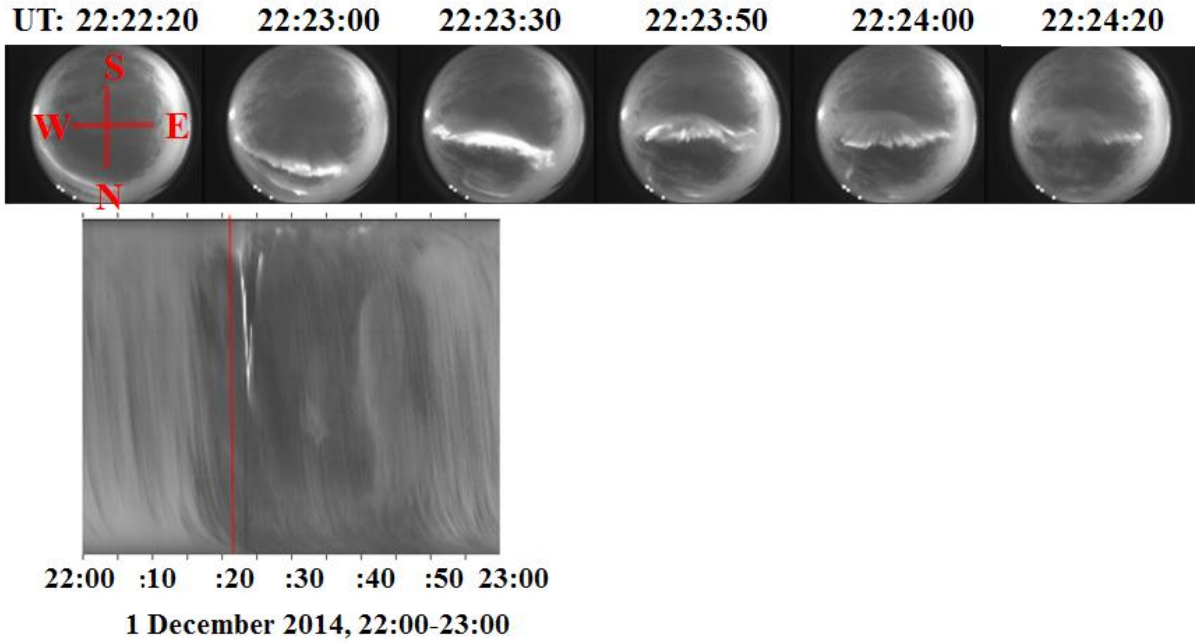

Figure 7. Auroras dynamics during the substorm on 01 December 2014 at 22:22:20 UT according to the all-sky camera data. The top panel shows some all-sky camera images taken during the substorm (from 22:22:20 to 22:24:20 UT). The bottom panel presents the all-sky keogram from 22:00 to 23:00 UT. The symbols and designations in Figure 7 are the same as the ones in Figure 2.

References:

Akasofu, S. - I.: 1964, Planet. Space Sci. 12, 273.

Despirak, I.V., Lubchich, A.A., Biernat, H.K., Yahnin, A.G.: 2008, Geomagn. Aeronomy 48(3), 284.

Despirak, I.V., Lyubchich, A.A., Kleimenova, N.G.: 2014, Geomagn. Aeronomy 54(5), 575.

Dmitrieva, N.P., Sergeev, V.A.: 1984, Magnitos. Issled. (in Russian) 3, 58–66.

Gerard, J.-C., Hubert, B., Grard, A., Meurant, M.: 2004, J. Geophys. Res. 109, A03208, doi: 10.1029/2003JA010129.

Guineva, V., Despirak, I., Kozelov, B.: 2016, Sun and Geosphere 11 (2), 101-105.

Gussenhoven M.S.: 1982, J. Geophys. Res. 87, 2401-2412.

Huttunen, K.E.J., Koskinen,H.E.J., Karinen, A.,Mursula, K.: 2006, Geophys. Res. Lett. 33, L06107, doi:10.1029/2005GL024894.

Kozelov, B.V., Pilgaev, S.V., Borovkov, L.P., Yurov, V.E.: 2012, Geosci. Instrum. Method. Data Syst. 1, 1.

Loomer, E.I., Gupta, J.C.: 1980, J Atmos. Sol.-Terr. Phys. 42, 645-652.

Maris, M.G., Besliu-Ionescu, D., Georgieva, K., Kirov, B.: 2014, 6th Workshop "Solar influences on the magnetosphere, ionosphere and atmosphere", 26-30 May 2014, Sunny Beach, Bulgaria, http://ws-sozopol.stil.bas.bg/.

McPherron, R.L., Russell, C.T., Kivelson, M.G., Coleman, P.J. Jr.: 1973, Radio Science 8, 1059-1076.

Nishida, A.: 1971, Cosmic Electrodynamics 2, 350.

Pulkkinen, T.I., Ganushkina, N.Y., Tanskanen, E.I., Kubyshkina, M., Reeves, G.D., Thomsen, M.F., Russel, C.T., Singer,H.J., Slavin, J.A., Gjerloev, J.: 2006, J. Geophys. Res. 111, A11S17, doi:10.1029/2006JA011627.

Tsurutani, B.T., Gonzalez, W.D., Gonzalez, A.L.C., et al.: 2006, J. Geophys. Res. 111, A07S01. doi: 10.1029/2005JA011273.

Tsurutani, B.T., Echer, E., Shibata, K., Verkhoglyadova, O.P., Mannucci, A.J., Gonzalez, W.D., Kozyra, J.U., Pätzold, M.: 2014, J. Space Weather Space Clim., 4, A02, DOI: 10.1051/swsc/2013056.

Yahnin, A.G., Despirak, I.V., Lyubchich, A.A., Kozelov, B.V.: 2004, in N. Ganushkina and T. Pulkkinen (ed.), Solar wind control of the auroral bulge expansion, Finnish Meteorological Institute, Helsinki, Finland, p. 31.

Yermolaev, Yu.I., Yermolaev, M.Yu.: 2006, Adv. Space Res. 37(6), 1175.